Latin American Journal of Solids and Structures
www.lajss.org

Experimental and Numerical Investigation of Perforation of Thin Polycarbonate Plate by Projectiles of Different Nose Shape

Abstract

The present study is based on experimental investigation and numerical simulation of impact of different nose shape projectiles on thin polycarbonate plates. Rigid hardened projectiles of two different geometries (Blunt and Truncated cone) keeping the same shank diameter and total mass were prepared. These projectiles were impacted through pneumatic gun setup on circular polycarbonate plates at varying impact velocities upto 106 m/s. Impact and residual velocities were measured before and after perforation, respectively. Numerical simulations were performed in ABAQUS/EXPLICIT finite element code. The problem has been modelled based on Mie-Gruneisen equation of state.

The experimental results obtained in terms of ballistic limit, residual velocity, energy absorbed and deformation mechanism have been compared with the numerical results and are found to be in excellent agreement. It is observed that the ballistic limit for normal impact is greater for blunt projectile compared to truncated conical projectile. Velocity drop and the energy absorbed is higher for blunt projectile compared to truncated conical projectiles for the impact velocities under study.

Keywords

Experimental; Ballistic; Polycarbonate; ABAQUS/Explicit; Subordnance velocity.

Afsar Husain
Raisuddin Ansari
Arshad Hussain Khan *

Department of Mechanical Engineering, Aligarh Muslim University, Aligarh 202001, U.P., India.
ahusain03@gmail.com,
braisansari@gmail.com,
khanahamu@gmail.com

* Corresponding author,
khanahamu@gmail.com;
ah.khan.me@amu.ac.in

http://dx.doi.org/10.1590/1679-78253252

Received 28.07.2016
In revised form 29.11.2016
Accepted 05.12.2016
Available online 09.12.2016

1 INTRODUCTION

Polycarbonate (PC) is a transparent material which offers high specific strength, good resistance to static and impact loads and as such found extensive application in optical lenses, automotive parts, house hold application, safety devices etc. and desired to act as protective structures against impact loading. The mechanism of penetration by a projectile and the associated damage characteristics should be analysed for the efficient design of PC structures. The maximum velocity of the projectile at which the complete perforation takes place with zero exit velocity referred to as ballistic limit

together with the modes of energy absorption in the deformation process can be utilised for the efficient design of the protective PC structures.

A number of investigations have been carried out to characterize the static/dynamic flow and failure properties of polycarbonate structures viz: Ravi-Chandar (1995); Rittel et al. (1997); Rittel and Levin (1998); Rittel (1999, 2000); Moisa et al. (2005); and Sarva et al. (2007). The penetration behavior of PC structures has been analysed by Wright et al. (1992), based on quasi-static deep penetration tests using circular cylindrical hardened steel punches. The resistance of thin PC plates (2, 5 and 12 mm thick) to impact by round and cylindrical projectiles was investigated experimentally by Wright et al. (1993). It is concluded that the five different modes of deformation are present i.e. elastic dishing, petalling, deep penetration, cone cracking and plugging. Inclined impact on thin PC plates (less than 6.4 mm thick) has also been investigated by Li and Goldsmith (1997), and it is concluded that the resulting perforated hole exhibits a much smaller diameter than the projectile, indicating a substantial capability for recovery. The ballistic resistance of clamped thin PC plates to single (Qasim and Yousif, 2008) and multiple ballistic impacts (Qasim, 2009) is analysed and it is concluded that reinforcements should be provided near the clamped edges.

The projectile geometry and the nose shape is an important factor affecting the mechanism of deformation of the target plates and relatively fewer studies are carried out to investigate their influence on metallic plates. Wingrove (1973) studied the influence of projectile geometry on aluminum alloy targets and concluded that blunt projectiles can penetrate more efficiently followed by hemispherical and ogive nosed projectiles, respectively, if the target thickness to projectile diameter ratio is less than one. Ipson et al. (1977) found that blunt projectiles penetrated the target more efficiently than conical projectiles when the thickness of target was moderate. For the case of thin and thick targets however, an opposite trend was observed.

It is evident from the literature survey that the influences of projectile geometry (nose shapes), impact velocities and target thickness on the impact behavior of PC plates has not been adequately analysed. The present work deals with experimental as well as numerical investigation of impact behavior of PC plates which can serve as benchmark for the efficient design of PC structures subjected to impact loading. The experimental analysis has been carried out using a Pneumatic gun setup with provisions of measurement of impact and residual velocities under normal/oblique impact. The projectiles of different geometries/nose shapes but of same material are manufactured and heat treated by keeping their mass and diameter constant achieved by varying the shank length.

A number of experiments are conducted to investigate the influences of nose shape and impact velocity and the performance parameters in terms of ballisitic limit, velocity drop, energy absorbed and deformation modes are investigated. Finite element simulation of the problem was carried out using finite element code ABAQUS. Residual velocities as well as the ballistic limit of the projectiles were obtained using the post processing module of the code. The predicted values of residual velocities were compared with the experiments and good correlation was found between the two. The predicted failure mechanism of the target plates is also found in good agreement with that observed experimentally.

2 EXPERIMENTAL ANALYSIS

Projectiles of two different nose shapes (Truncated cone and Blunt) of 12.8 mm diameter and 25.8 g mass are used in the experiments. Projectiles of the required shapes are machined from EN-31 alloy

and they are heat treated by raising the temperature to 920 °C. Subsequently oil quenching is done at room temperature for obtaining the desired hardening of the projectiles. The hardened projectiles is then tested on Rockwell hardness testing machine and it is found that the hardness of the projectiles correspond to 64-65 Rh (Rockwell hardness number). The hardness is brought to the desired range of 47- 50 Rh by tempering. The dimensions and final shape of the projectiles are shown in Fig. 1. The projectiles were so designed that their mass remains same which is achieved by varying the shank length of the projectiles and keeping their diameter same.

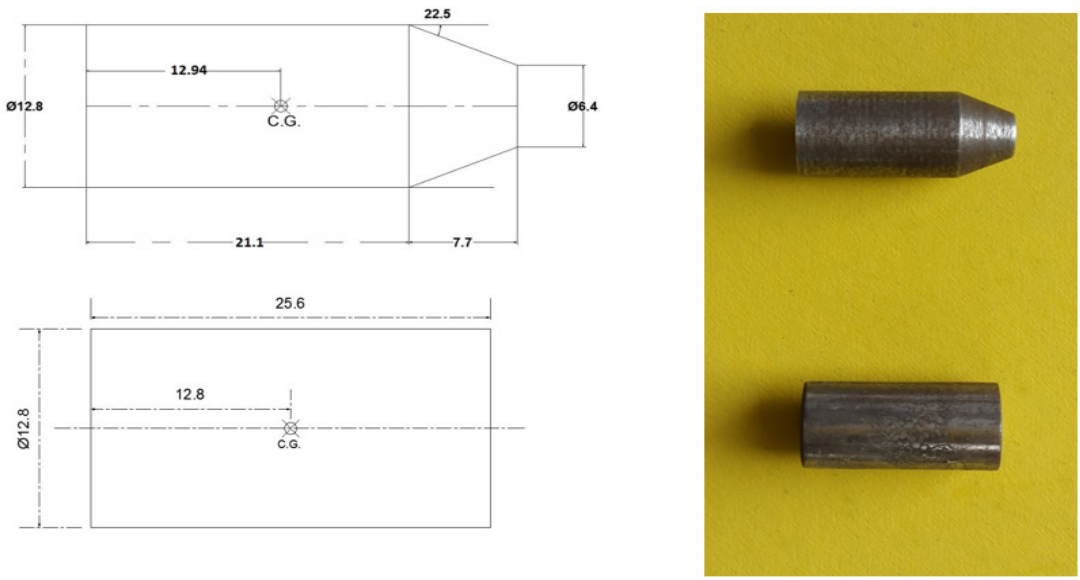

Figure 1: Schematics and camera view of Truncated cone and Blunt projectile.

The mechanical properties of the target (PC) plate is evaluated from the tensile test on UTM. A standard tensile specimen as per ASTM standards is cut from PC plate to evaluate the properties of PC. Stress strain diagram of PC is shown in Fig. 2 and the evaluated properties are tabulated in Table 1. Circular target plate of PC whose mechanical properties have been evaluated is shown in Fig. 3. The thickness of the plate is 2.66 mm and the outer diameter is 255 mm. In order to rigidly secure the target PC plate for impact testing on the pneumatic gun setup eight holes are drilled at pitch circle of 230 mm diameter. The effective diameter of target plate is 205mm.

The schematics and the pictorial view of the Pneumatic gun-setup is shown in Fig. 4 which is employed for impact testing. Pneumatic gun setup consist of a pressure source, regulator, pressure chamber, projectile chamber, barrel, optical fibre sensor for measuring the impact velocity, dual screen of aluminium foil for measuring the residual velocity of projectile. The impact velocity in the experiment is varied between 65 m/s to 106 m/s. Impact energy is calculated by calculating the kinetic energy of the projectile ($E_i = 0.5*m*v^2$) where m is the mass of projectile and v is the impact velocity of the projectile. Residual energy is calculated by substituting the measured residual velocity in the

same equation. The energy absorbed is calculated by taking the difference of impact energy and residual energy.

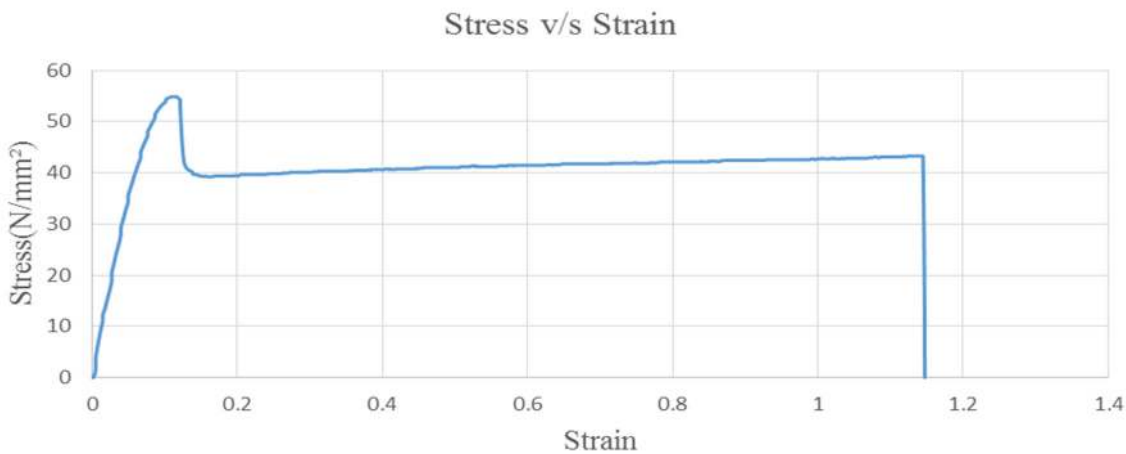

Figure 2: Stress-strain diagram of polycarbonate.

Youngs modulus E (N/mm^2)	2000
0.2% offset Yield Stress (N/mm^2)	55
Elongation at Peak (%)	10.9
Elongation at Break (%) (Total Elongation)	114.7

Table 1: Results of stress v/s strain graph.

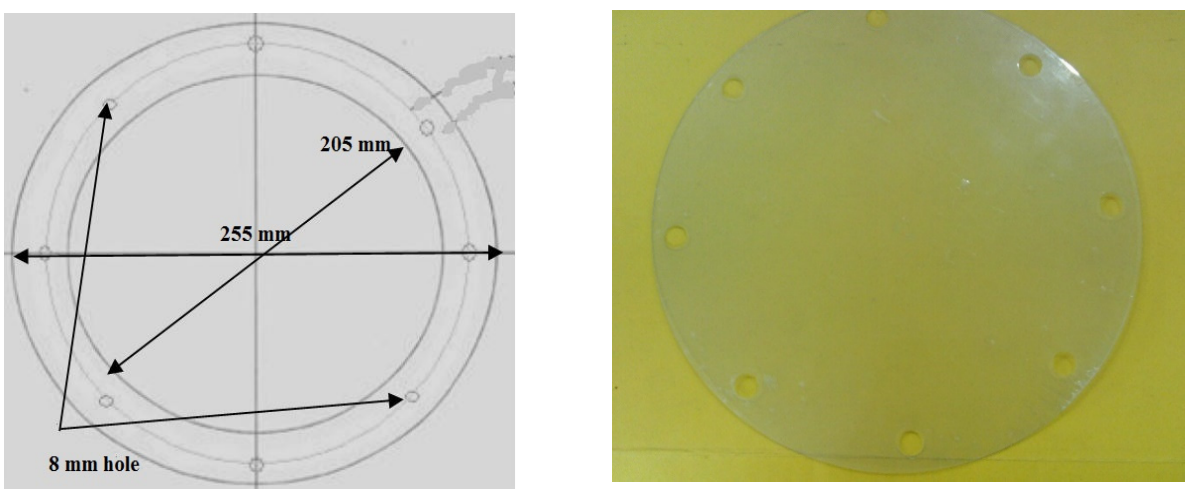

Figure 3: Schematic and camera view of target plate.

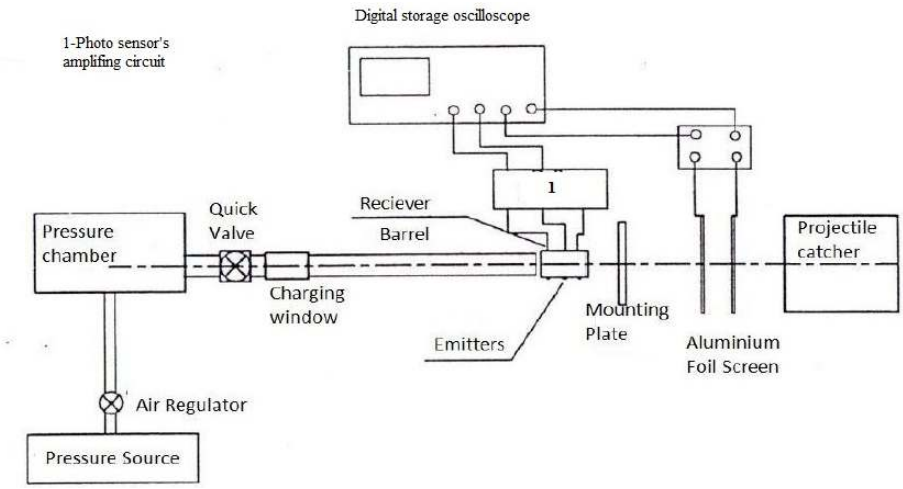

Figure 4: Schematic diagram of the Pneumatic gun setup.

3 NUMERICAL ANALYSIS

The finite element analysis is carried out based on axi-symmetric model on ABAQUS CAE. Axi-symmetric analytically rigid projectiles were modelled as per the geometry employed in the experiments. The projectile is given a reference point at center of gravity of the whole body. The plate is modeled as axi-symmetric deformable body with shell feature and two partitions were constructed on it. The first partition was supposed to be an impact zone, at center, where the projectile has actually made contact with the plate, the second partition was made to observe the local deformation, around the impact zone. The projectile and plate is being assembled together along the axis of symmetry line as shown in Fig. 5. The projectile was initially kept a little away from the plate, to notice its first indentation.

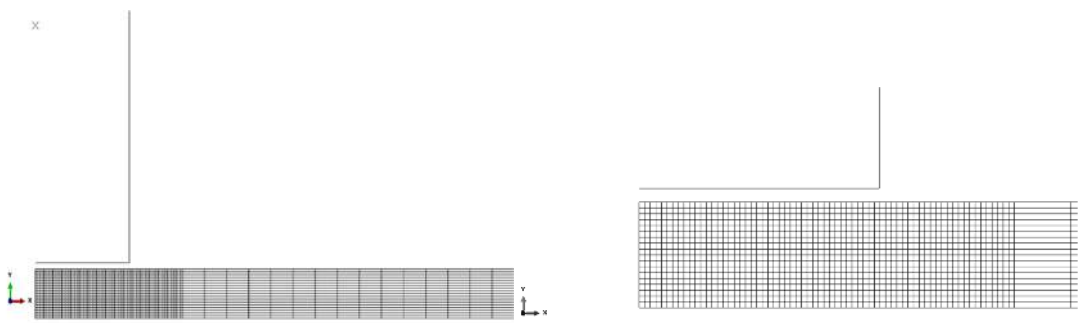

Figure 5: Plate partition and its enlarged view.

The polycarbonate plate has been modeled based on Mie-Grüneisen equation of state (EOS) with application of linear Us-Up Hugoniot. Us is the linear shock wave and Up is the particle speed (Dorogy et.al., 2011). This model can be applied to materials which also have isotropic elastic or viscous deviatoric behavior. It is used with a Mises plasticity model.

The Mie- Grüneisen equation of state is linear in energy and can be represented by

$$p - p_H = \Gamma\rho(E_M - E_H) \tag{1}$$

where p_H and E_H are the Hugoniot pressure and specific energy (per unit mass) and are functions of density (ρ) only, and Γ is the Grüneisen ratio defined as

$$\Gamma = \Gamma_0 \frac{\rho_0}{\rho} \tag{2}$$

where Γ_0 is a material constant and ρ_0 is the reference density.

The Hugoniot energy, E_H is related to the Hugoniot pressure by

$$E_H = \frac{p_H \eta}{2\rho_0} \tag{3}$$

where $\eta = 1 - \frac{\rho_0}{\rho}$ is the nominal volumetric compressive strain. Elimination of Γ and E_H from the above equations yields

$$p = p_H\left(1 - \frac{\Gamma_0\eta}{2}\right) + \Gamma_0\rho_0 E_M \tag{4}$$

The equation of state and the energy equation represent coupled equations for pressure and internal energy. These equations are solved simultaneously at each material point by Abaqus/Explicit solver.

The Hugoniot pressure p_H, is a function of density only. A common fit to the Hugoniot data is given by:

$$p_H = \frac{\rho_0 c_0^2 \eta}{(1 - s\eta)^2} \tag{5}$$

where c_0 and s define the linear relationship between the linear shock velocity, Us and the particle velocity, Up, as follows:

$$U_s = c_0 + sU_p \tag{6}$$

With the above assumptions the linear $Us - Up$ Hugoniot form is written as

$$p = \frac{\rho_0 c_0^2 \eta}{(1 - s\eta)^2}\left(1 - \frac{T_0\eta}{2}\right) + \Gamma_0\rho_0 Em \tag{7}$$

where $\rho_0 c_0^2$ is equivalent to elastic bulk modulus at small nominal strains. There is a limiting compression given by the denominator of this form of the equation of state

$$\eta_{lim} = \frac{1}{s} \text{ or } \rho_{lim} = \frac{s\rho_0}{s-1} \tag{8}$$

The hydrodynamic material data for the polycarbonate was taken from Dorogy et.al. (2011) and is confirming to the AUTODYN material libraries. The properties of the polycarbonate is summarized in Table 1 while the physical properties and hydrodynamic data for the polycarbonate are given in Table 2. The strain-rate and temperature dependence of the plastic behavior is shown in Fig. 6. The strain rate dependence is based on experimental results with cylindrical specimens (Rittel and

Dorogoy, 2008), which uses a linear extrapolation for plastic strains up to 1. The strain stress curve for strain rates is assumed to be identical to that of 8000 1/s. It was assumed that at T=100°C for all strain rates, the PC softens and the yield stress is half of the quasi-static one, while at T=200°C it drops almost to zero, and the material flows freely (Bauwens et al., 1972). The damage initiation values are specified in Table 3. These values are based on experimental results obtained by torsional split Hopkinson bar (Fleck et al., 1990) in which fracture occurred at shear strain $1.5 < \gamma < 2.0$. The linear displacement damage evolution value used is 80 mm, which was also used for PMMA in Dorogoy et al. (2010).

Density ρ [Kg/m^3]	1200
Specific Heat [J/Kg.K°]	1300
Inelastic heat fraction	1
Reference density ρ_o [Kg/m^3]	1910
Bulk sound speed c_o [m/s]	1933
Slope s in Us versus Up diagram	2.65
Gruneisen coefficient Γ_o	0.61

Table 2: Physical property and Hydrodynamic data for the polycarbonate (Dorogy et al., 2011).

Strain rate [1/s]	Polycarbonate
Quasi static	1.0
4900	0.85
8000	0.85
80000	0.60
Damage evolution [µm]	80

Table 3: Damage initiation values and damage evolution for polycarbonate (Fleck et al., 1990).

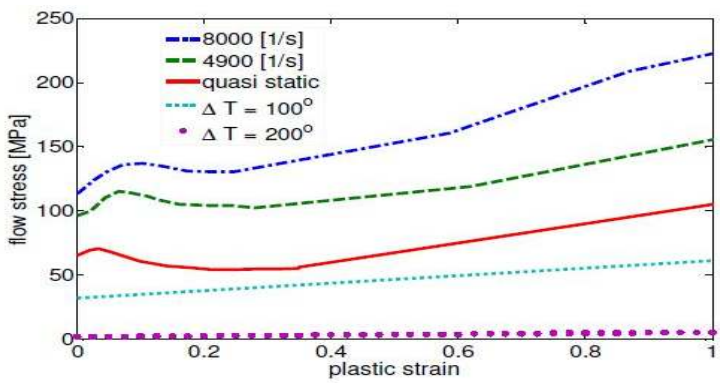

Figure 6: Plastic properties of polycarbonate used in modelling polycarbonate (Rittel and Dorogoy, 2008).

Meshing is done on polycarbonate plates of 2.66 mm thickness by using CAX4R (4-node bilinear axisymmetric quadrilateral, reduced integration, hourglass control) such that the results can be achieved accurately with minimum computational time. The surface to surface contact between the projectile and target plate was modeled using kinematic contact algorithm with finite sliding formu-

lation. The penetration of slave nodes into the master surface is eliminated at the end of each increment. The projectile was considered as the master surface and the impact region of the plate is modelled as node based slave surface. The frictional effect between the plate and projectile is assumed negligible because of small thickness of the plate. The number of elements chosen for the discretization of polycarbonate plate is based on mesh convergence.

A mesh sensitivity analysis has been carried out to confirm that the results obtained are not sensitive to mesh size. Blunt projectile impacting the polycarbonate plate with an impact velocity of 88.24 m/s is considered. Eight different mesh sizes by varying the number of element from 12 to 19 (element length from 0.22 to 0.15 mm, respectively) are considered and the results for residual velocity corresponding to each mesh size is presented in Table 4 and the convergence is plotted in Fig. 7. Aspect ratio is the number of elements taken along the length to the number of elements along the thickness direction. When this ratio approaches unity, Zukas et al. (2000) suggested that simulation approaches its real values. The numbers of elements were varied along the thickness direction from 12 to 19 and aspect ratio of the elements was kept close to unity. The condition for a unity aspect ratio is recommended (as some dependency upon the mesh does remain) but is not essential, as we are using the damage initialization and damage evolution criteria for defining damage. The predicted numerical value of the residual velocity for different number of elements is also compared with the experimental residual velocity and the results have been plotted in Fig. 7. It can be seen that the solution converges for 18 number of elements with element length equal to 0.15 mm. Hence the number of element choosen for the numerical analysis is 18.

No of Element (n)	Element size (mm^2)	Residual velocity (m/s)
12	0.22x0.22	29.44
13	0.21x0.21	29.22
14	0.19x0.19	32.51
15	0.18x0.18	33.18
16	0.17x0.17	33.51
17	0.16x0.16	33.87
18	0.15x0.15	35.90
19	0.14x0.14	35.91

Table 4: Mesh convergence and element size.

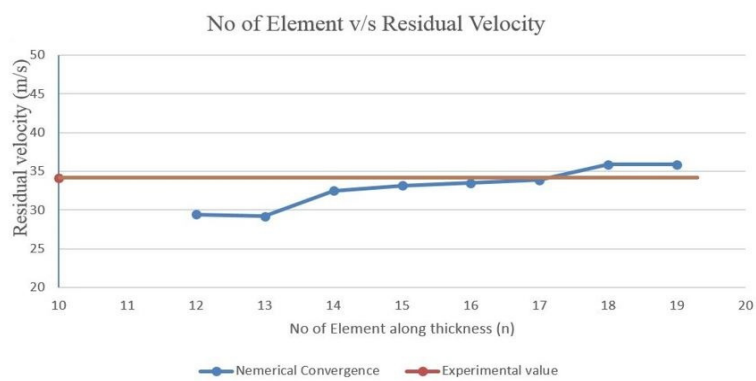

Figure 7: Number of Element along thickness v/s Residual velocity.

The ballistic limit is estimated based on the U.S. military standard (MIL-STD-662E, 1987). This standard defines the ballistic limit by taking the average of equal number of highest partial penetration velocities and lowest complete penetration velocities which occur within a specific range. The ballistic limit has been estimated from present FE model from velocity time histories, for an initial impact velocity at the stage when the residual velocity reaches close to zero. The ballistic limit velocity obtained from FE analysis and experimental predictions are found to be in excellent agreement. The above validation implies that the present FE model is capable of simulating the ballistic impact response of Polycarbonate target.

4 RESULTS AND DISCUSSION

(a) Normal Impact of Blunt Projectile

The ballistic performance of the PC plate has been evaluated by calculating the percentage of energy absorbed by the target and residual velocities. A number of experiments on polycarbonate plates of thickness 2.66 mm were carried out to study the response of the plates subjected to normal impact of blunt projectile. Impact velocity of the projectile is varied from 76 m/s to 106 m/s and the numerical simulation is also carried out in the same velocity range. The geometry of the target, projectile and the boundary conditions remain same. The mode of deformation of the PC plate after impact through the pneumatic gun setup at different velocities is shown in Fig. 8. It is observed from the experimental investigations that the plug remains attached to the plate below 100m/s. The experimental results obtained in terms of residual velocity, absorbed energy and residual energy are tabulated in Table 5 whereas the numerical results obtained from simulation in ABAQUS are presented in Table 6. The comparison of the experimental results with the numerical results reveal close agreement between the two. The comparison of the back face signature of the perforated plate shown in Fig. 9, reveal similar kind of burr in the plate end and the shape of the plug is similar in experimental as well as simulated results.

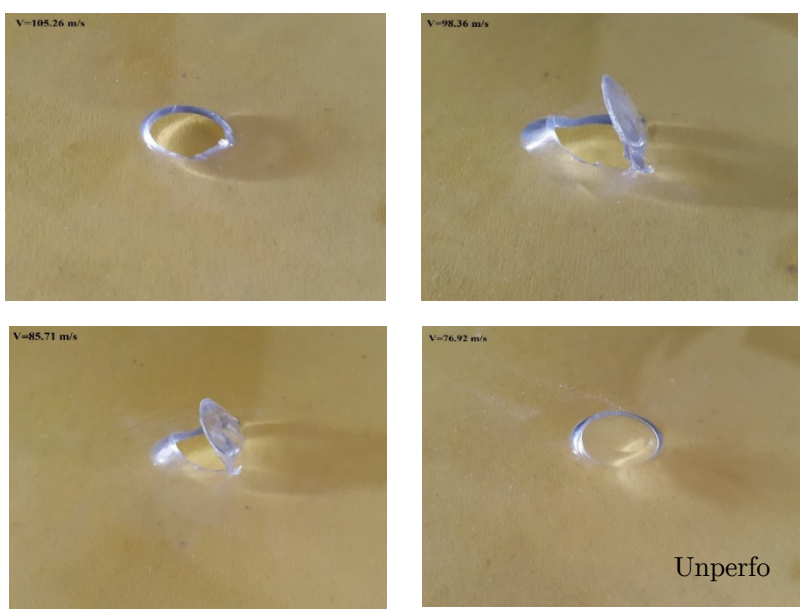

Figure 8: Deformed shape of polycarbonate plates under normal impacted by Blunt projectile at different velocities.

S.No	Specimen No	Impact Velocity (m/s)	Residual Velocity (m/s)	Velocity Drop (m/s)	Impact Energy (J)	Residual Energy (J)	Absorbed Energy (J)
1	BP1	106.19	64.25	41.94	143.77	52.63	91.14
2	BP7	105.26	62.15	43.11	141.27	49.25	92.02
3	BP8	101.69	55.23	46.46	131.85	38.89	92.95
4	BP2	98.36	49.79	48.57	123.35	31.61	91.74
5	BP4	88.24	34.12	54.12	99.28	14.84	84.43
6	BP6	85.71	0	85.71	93.66	0	93.66
7	BP5	76.92	N.P.				

N.P. – Plate is not perforated

Table 5: Experimental results of Blunt projectile on polycarbonate plate.

S.No	Impact Velocity (m/s)	Residual Velocity (m/s)	Velocity Drop (m/s)	Impact Energy (J)	Residual Energy (J)	Absorbed Energy (J)
1	106.19	67.02	39.17	143.77	57.27	86.50
2	105.26	65.52	39.74	141.27	54.73	86.53
3	101.69	59.99	41.70	131.85	45.88	85.96
4	98.36	53.16	45.20	123.35	36.03	87.32
5	88.24	35.90	52.34	99.28	16.43	82.84
6	85.71	2.5	83.21	93.66	0.08	93.58
7	76.92	N.P.				

N.P. – Plate is not perforated

Table 6: Numerical result of Blunt projectile on polycarbonate plate.

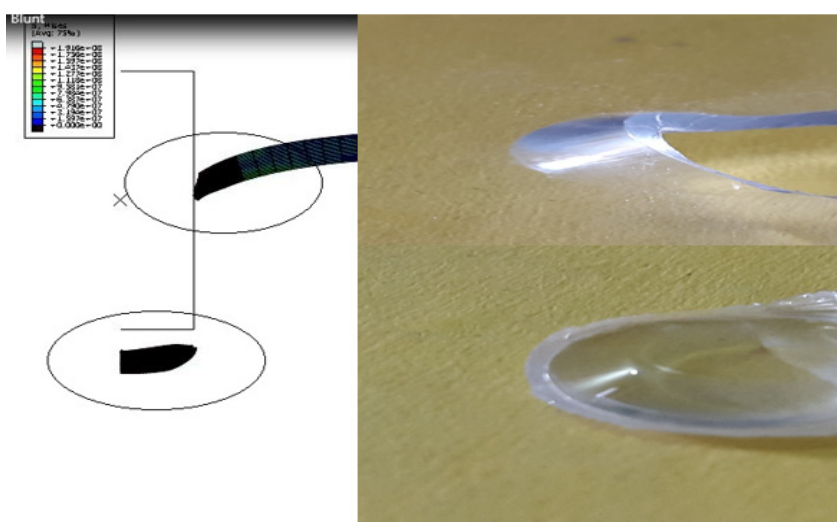

Figure 9: Comparison of back face signature of perforated plate obtained from experiment/simulation for blunt projectile.

(b) Normal Impact of Truncated Cone Projectile

In order to analyse the influence of nose shape on the impact response of polycarbonate plates of thickness 2.66 mm a number of experiments were carried out using truncated cone projectile. The shape of the projectile is changed without altering its diameter and mass by varying the shank length. Impact velocity is varied from 65 m/s to 105 m/s and numerical simulation is also carried out in the same velocity range. The deformed configuration of the PC plate obtained experimentally after impact at different velocities is shown in Fig.10. It can be seen that the plug remains attached to the plate below the impact velocity of 100 m/s. A detailed parametric analysis is carried out and the experimental results pertaining to residual velocity, velocity drop and residual/absorbed energies corresponding to different impact velocities of the truncated cone projectiles are tabulated in Table 7. The numerical results obtained by simulation using ABACUS-CAE are presented in Table 8. The comparison of the experimental and simulation results shown in Table 7 & 8, reveal excellent agreement between the two. The deformed configuration and the back face signature of the perforated plate obtained from experiments and numerical simulation are compared in Fig. 11,which shows a similar kind of deformation pattern and the shape of the plug is similar in both the analysis i.e. the plug is thin at the ends from both side.

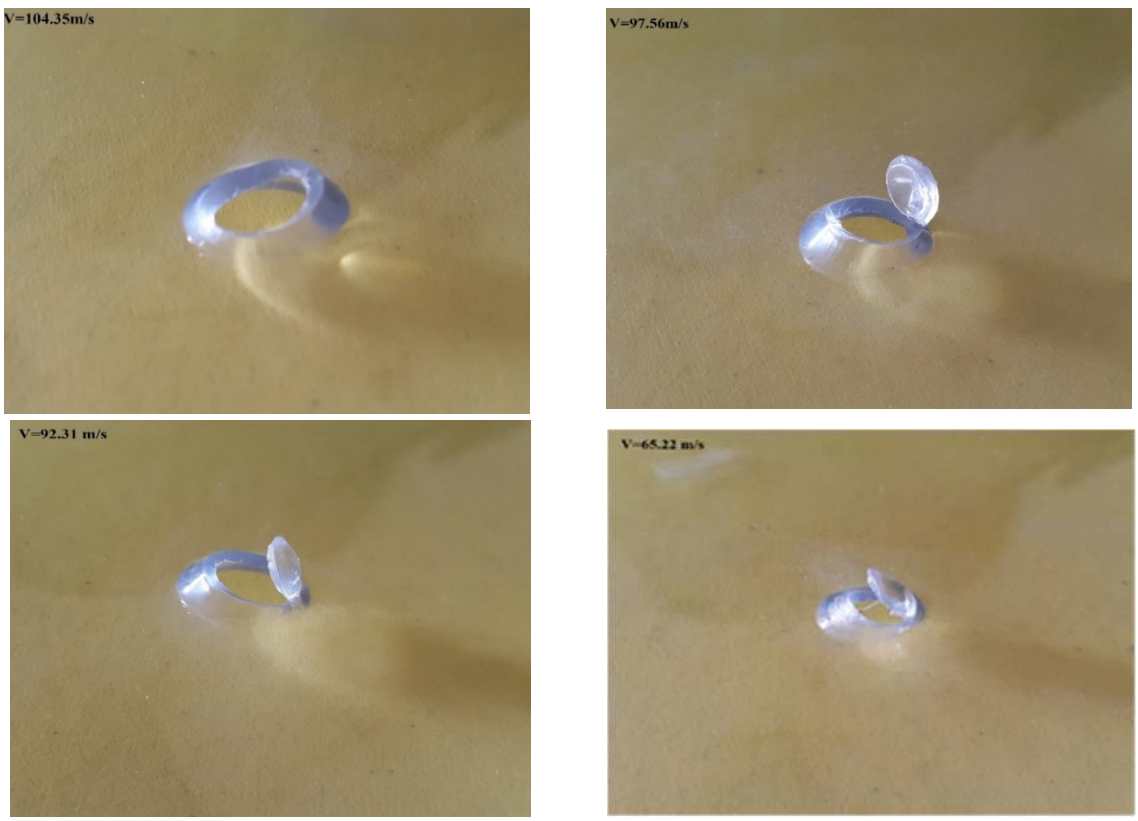

Figure 10: Deformed shape of polycarbonate plates impacted by Truncated Cone projectile at different velocities.

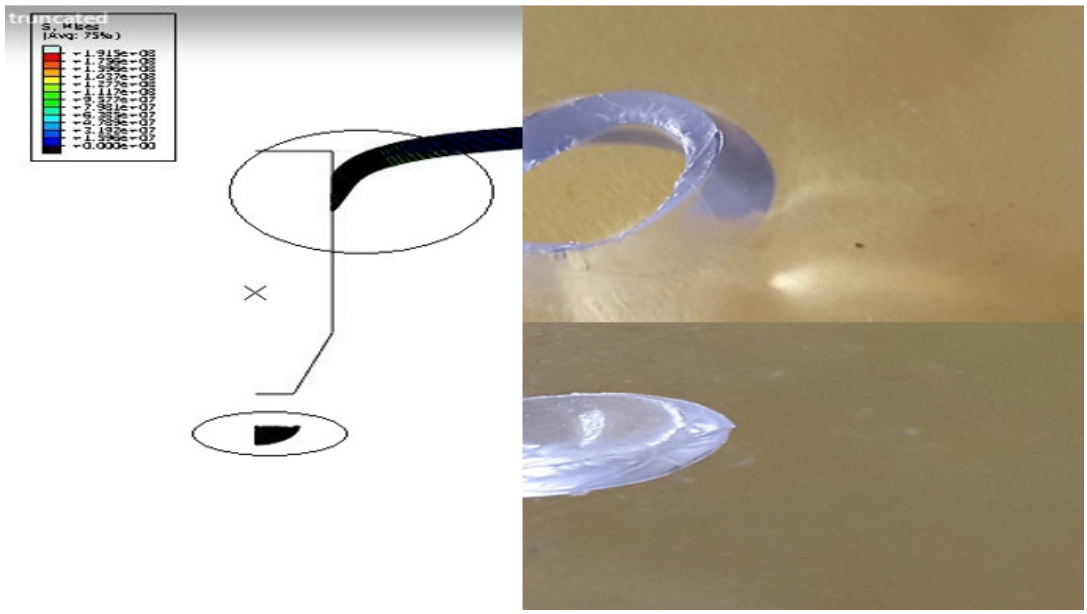

Figure 11: Comparison of back face signature of perforated plate from experimental/simulation for truncated cone projectile.

S.No	Specimen No.	Impact Velocity (m/s)	Residual Velocity (m/s)	Velocity Drop (m/s)	Impact Energy (J)	Residual Energy (J)	Absorbed Energy (J)
1	TP2	104.35	62.2	42.15	138.83	49.33	89.51
2	TP3	97.56	57.19	40.37	121.35	41.70	79.65
3	TP5	92.31	48.95	43.36	108.64	30.55	78.09
4	TP4	91.6	48.55	43.05	106.98	30.05	76.93
5	TP6	85.11	47.19	37.92	92.36	28.39	63.96
6	TP7	76.43	31.44	44.99	74.48	12.60	61.88
7	TP8	65.22	0	0	54.23	0	54.23

Table 7: Experimental result of Truncated Cone projectile on polycarbonate plate.

S.No	Impact velocity (m/s)	Residual Velocity (m/s)	Velocity Drop (m/s)	Impact Energy (J)	Residual Energy (J)	Absorbed Energy (J)
1	104.35	67.76	36.59	138.83	58.54	80.29
2	97.56	60.91	36.65	121.35	47.30	74.05
3	92.31	51.94	40.37	108.64	34.40	74.05
4	91.6	50.61	40.99	106.98	32.66	74.32
5	85.11	48.12	36.99	92.36	29.52	62.83
6	76.43	27.56	48.87	74.48	9.68	64.80
7	65.22	N.P.	62.72	54.23	0.08	54.15

N.P. – Plate is not perforated

Table 8: Numerical result of Truncated Cone projectile on polycarbonate plate.

(c) Effect of Nose Shape on the Response Parameters

The influence of the nose shape on the residual velocity for different impact velocities is shown in Fig. 12. It can be inferred from the figure that the residual velocity is nearly same for blunt as well as truncated cone projectiles at higher impact velocities however at impact velocities up to 100 m/s, the residual velocity for truncated cone projectile is significantly greater than that for blunt projectile. It has been observed that the truncated cone projectile has perforated the PC plate at much lower impact velocity compared to blunt projectile.

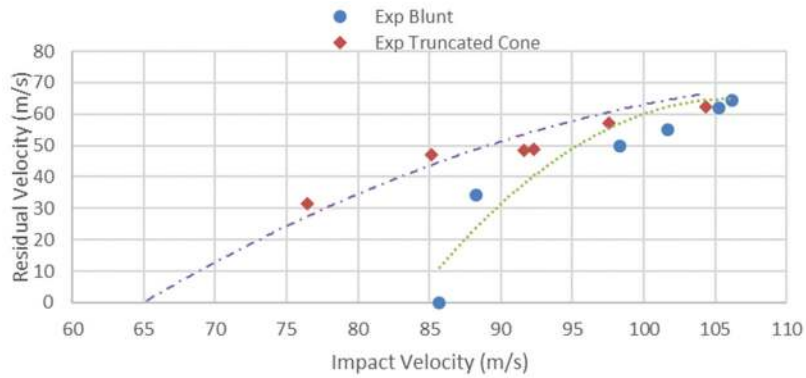

Figure 12: Variation of the residual velocity for different nose shape projectile.

Figure 13 shows the variation of the velocity drop with increasing impact velocities by different projectiles. At lower impact velocities, it is observed that the velocity drop is more for blunt projectiles compared to truncated cone projectile.

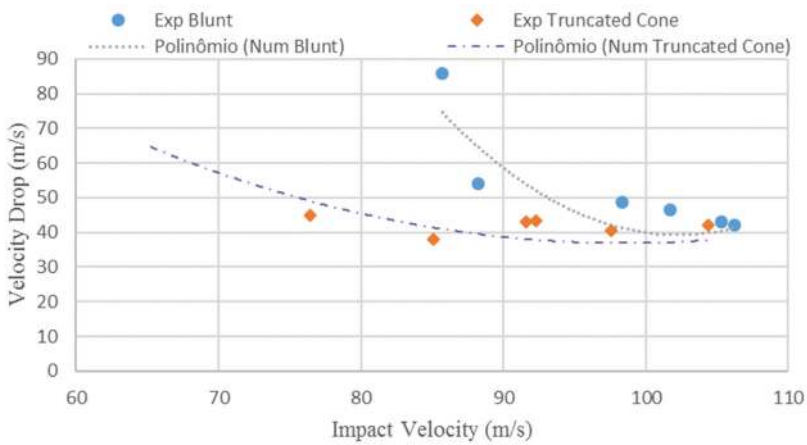

Figure 13: Variation of the velocity drop for different nose shape projectile.

The variation of energy absorbed with impact energy for blunt/truncated cone projectiles is shown in Figure 14. The Energy absorbed at higher impact energy is almost same for both projectile shapes but there is large variation in energy absorbed at low impact energy. For Blunt projectile energy

absorbed is more at lower impact energy compared to truncated cone projectile. The effect of nose shape is more prominent at low impact energy. This is because of greater contacting area as well as larger shearing area for blunt projectile compared to conical projectile. Further the global deformation (dishing) is large (refer Fig. 16) at lower impact velocity resulting in larger energy absorption for blunt projectiles compared to conical projectiles.

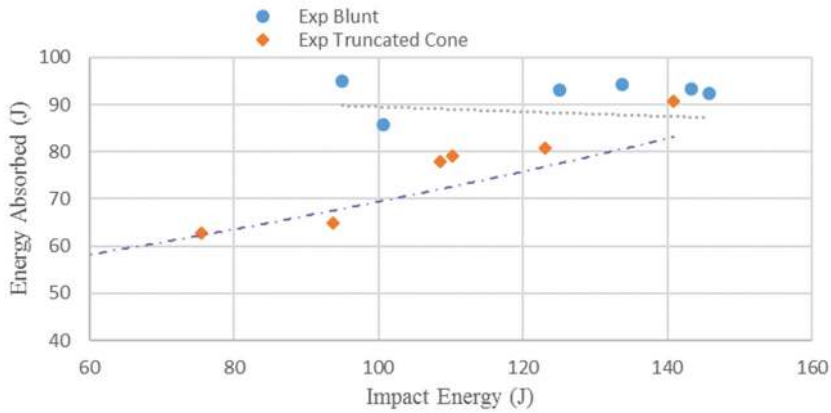

Figure 14: Variation of the energy absobed for different nose shape projectile.

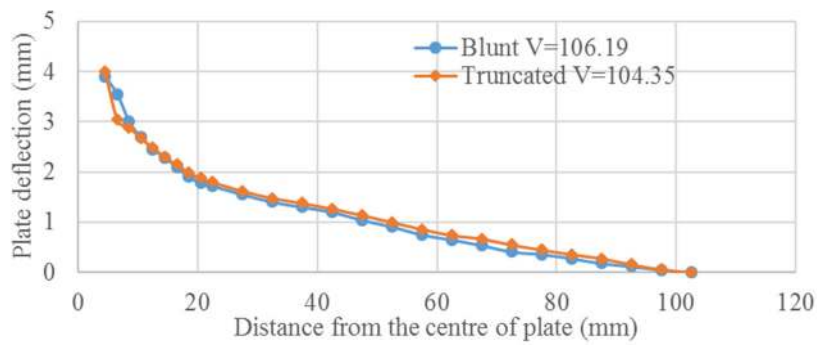

Figure 15: Plate profile for impact velocity greater than 100 m/s.

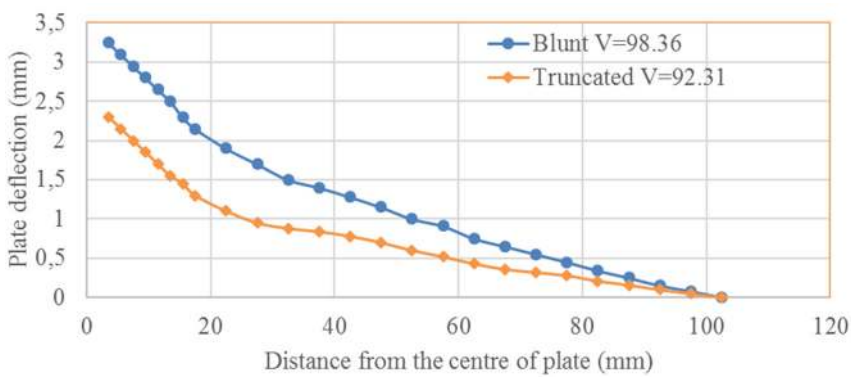

Figure 16: Plate profile for impact velocity below 100 m/s.

The local/global deformation pattern (plate profile) obtained experimentally during the normal impact of blunt and truncated cone projectiles at different impact velocities are shown in Fig.'s 15-16. It can be seen from Fig. 15 that for impact velocity greater than 100 m/s the global deformation or dishing and local deformation or bulging are same for both blunt as well as truncated cone projectile. However, for impact velocity below 100 m/s greater bulging is observed in truncated cone projectile which may be attributed to half conical shape of the projectile (Fig. 16). Around the periphery of the deformed plate dishing (global deformation) is same for both blunt and truncated cone projectiles however as we move towards the center from the periphery both dishing as well as bulging (local deformation) is greater for truncated cone projectiles as compared to blunt projectile.

4 CONCLUSIONS

The response of polycarbonate plate subjected to normal impact by Blunt and Truncated cone projectiles in the sub ordnance velocity range has been analyzed experimentally as well as by axi-symmetric numerical simulations using ABAQUS-CAE. The present analysis can be used as a benchmark for designing protective equipment's/components subjected to impact loading. Based on the detailed investigations the following conclusions can be drawn:

i. The ballistic limit of 2.66 mm thick polycarbonate plate for normal impact of blunt and truncated-cone projectile is found to be 81.32 m/s and 70.83 m/s, respectively. The values obtained experimentally are found to be in close proximity with the simulation results.
ii. The plug remains attached from the plate in both type of projectiles (blunt and truncated cone) at impact velocities below 100 m/s.
iii. At higher impact velocities greater than 100 m/s the velocity drop for both the projectiles is found to be almost same. This may be due to the fact that plug starts detaching after this velocity and shearing force is applied to all the circumference of petal to detach it from the plate completely.
iv. The velocity drop increases rapidly at higher impact velocity and the rate of increase is more in blunt projectile as compared to truncated cone projectile.
v. Energy absorbed is more in blunt projectile as compared to truncated cone projectile.
vi. For impact velocity less than 100 m/s greater bulging is observed in truncated cone projectile which may be attributed to half conical shape of the projectile.

Acknowledgement

The authors acknowledge the financial support from DST-PURSE, Government of India.

References

Abaqus/CAE version 6.9-EF1. (2009), Abaqus documentation. Abaqus Analysis User's manual, chapters 20- 22, Dassault systemes. New York: Springer.

Bauwens-Crowet, C., Bauwens, J.C., Homes, G. (1972), The temperature dependence of yield of polycarbonate in uniaxial compression and tensile tests. J Mater Sci.; 7: 176-183.

Dorogoy, A., Rittel, D., Brill, A. (2010), A study of inclined impact in polymethyl methacrylate plates. Int J Impact Eng ;37: 285-94.

Dorogy, A., Rittel, D., Brill, A. (2011), Experimentation and modeling of inclined ballistic impact in thick polycarbonate plates. Int J Impact Engg.; 38: 804-814.

Fleck, N.A., Stronge, W.J., Liu, J.H. (1990), High strain-rate shear response of polycarbonate and polymethyl methacrylate. Proc R Soc Lond A; 429:459e79.

Ipson, T.W., Recht, R.F. (1977), Ballistic Perforation by Fragments of Arbitrary Shape, NWC TP 5927. Denver Research Institute,Naval Weapons Centre, China Lake, CA, USA.

Li, K., Goldsmith, W. (1997), Perforation of steel and polycarbonate plates by tumbling projectiles. Int J Solids Struct; 34: 35-36: 4581-4596.

Military Standard V50 Ballistic Test for Armor (1987), MIL-STD-662E.

Moisa, S., Landsberg, G., Rittel, D., Halary, J.L. (2005), Hysteretic thermal behavior of amorphous semi-aromatic polyamides. Polym J ; 46: 25: 11870-11875.

Qasim, H.S., Yousif, A.A. (2008), Effect of distance from the support on the penetration mechanism of clamped circular polycarbonate armor plates. Int J Impact Eng; 35: 11: 1244-1250.

Qasim, H.S. (2009), Impact resistance of a rectangular polycarbonate armor plate subjected to single and multiple impacts. Int J Impact Eng; 36:9: 1128-1135.

Ravi-Chandar, K. (1995), On the failure mode transitions in polycarbonate under dynamic mixed mode loading. Int J Solids Struct; 32: 6-7: 925-938.

Rittel, D., Dorogoy, A. (2008), A methodology to assess the rate and pressure sensitivity of polymers over a wide range of strain rates. J Mech Phys Solids.; 56: 3191–3205

Rittel, D., Levin, R., Maigre, H. (1997), On dynamic crack initiation in polycarbonate under mixed mode loading. Mech Res Commun; 24: 1: 57-64.

Rittel, D., Levin, R. (1998), Mode-mixity and dynamic failure mode transitions in polycarbonate. Mech Mater: 30: 3: 197-216.

Rittel, D. (1999), On the conversion of plastic work to heat during high strain rate deformation of glassy polymers. Mech Mater; 31: 2: 131-139.

Rittel, D. (2000), Experimental investigation of transient thermoplastic effects in dynamic fracture. Int J Solids Struct; 37: 21: 1 : 2901-2913.

Sarva, S., Mulliken, A.D., Boyce, M.C. (2007), Mechanics of Taylor impact testing of polycarbonate. Int J Solids Struct; 44: 7-8: 2381-2400.

Wingrove, A.L. (1973), The influence of projectile geometry on adiabatic shear and target failure. Metallurgical Transactions A 4, 1829–1833.

Wright, S.C, Fleck, N.A., Stronge, W.J. (1993), Ballistic impact of polycarbonate—An experimental investigation. Int J Impact Eng; 13: 1: 1-20.

Wright, S.C., Huang, Y., Fleck, N.A. (1992), Deep penetration of polycarbonate by a cylindrical punch. Mech Mater; 13: 4: 277-284.

Zukas, J.A., Scheffler, D.R. (2000), Practical aspects of numerical simulations of dynamic events: effects of meshing. Int J Impact Engg.; 9: 925–45.